

# SIW Rotman Lens with Planar Slot Array Antenna at Ku-band

S. A. Hosseini, Z. H. Firouzeh, and M. Maddahali

Dept. of Electrical and Computer Engineering  
Isfahan University of Technology, Isfahan, 8415683111, Iran  
Alireza.hosseini@ec.iut.ac.ir, Zhfirouzeh@cc.iut.ac.ir, Maddahali@cc.iut.ac.ir

**Abstract** — A multi-beam antenna, which is the combination of a Rotman lens and a planar slot array antenna, is designed in this paper. The lens and the slot array are designed for 15.5 to 16.5 GHz frequency range and implemented in the same substrate using SIW structure. The Rotman lens with 7 input ports and 7 output ports are connected to a planar slotted array antenna with 7 waveguides. This multi-beam antenna consists of seven beams at angles of  $0^\circ$ ,  $\pm 10^\circ$ ,  $\pm 20^\circ$  and  $\pm 30^\circ$  symmetrically. This antenna is designed for terrestrial and satellite applications, where the low cost, low profile and light multi-beam antennas are needed. Simulated and measured results show that the amplitude and phase distributions and scattering parameters of the antenna are in good agreement. In addition, the SLL, HPBW, main beam direction and cross polarization levels of all the radiation patterns are desirable.

**Index Terms** — Beam steering, Rotman lens, slot array antenna, Substrate Integrated Waveguide (SIW).

## I. INTRODUCTION

Multi-beam antennas are used to produce several independent beams at different angles simultaneously or individually. Such antennas are widely used in terrestrial communications, including wireless, MIMO, direction finding, and in satellite communications such as MSS and BSS services [1]. Beamforming that accomplished using an array antenna and a beamforming network (BFN) is one way to realize multiple beams. Beamforming can be implemented by analog [2] and digital methods [3].

In analog BFNs the phase and amplitude distribution of array is controlled by a network of power dividers and phase shifters or transmission lines. There is no need to employ microprocessors and processing algorithms in analog BFNs; therefore these beamformers are simpler, cheaper and lighter than digital types, and are more suitable for some terrestrial and satellite applications. Butler matrix and microwave lenses [2] are some examples of analog BFNs. Rotman lens [4] is the best and most popular lens among microwave lenses, because of its simplicity, compactness, true time delay

characteristic and ability of attaching to the linear arrays.

Rotman lens that invented first by Rotman and Turner [4], is a multi-input multi-output network and as can be seen in Fig.1, all of its ports are connected to a parallel plate region. By connecting the output ports of Rotman lens to the array element through transmission lines, a multibeam antenna is realized. In this antenna, by exciting each input port, a particular amplitude and phase distribution is created on array elements which led to the creation of a beam at a specific angle of space. Rotman lens has the superposition property, so each beam can be individually turned on or off.

Substrate Integrated Waveguide (SIW) Rotman lens is a new type of lenses that has been developed in recent years [5, 6], and compared with other types of Rotman lenses, a little works have been devoted to it. This lens has desirable features of microstrip [7] and waveguide lenses [8] simultaneously, and can be integrated with some kind of widely used arrays such as SIW slot array antenna. Thus, the purpose of this paper is to provide a Rotman lens with a slot array antenna based on SIW structure. It should be noted that the design equations vary based on the type of Rotman lens such as microstrip, waveguide, SIW and so on. The design methods and equations of SIW Rotman lens have been reported in [5, 9].

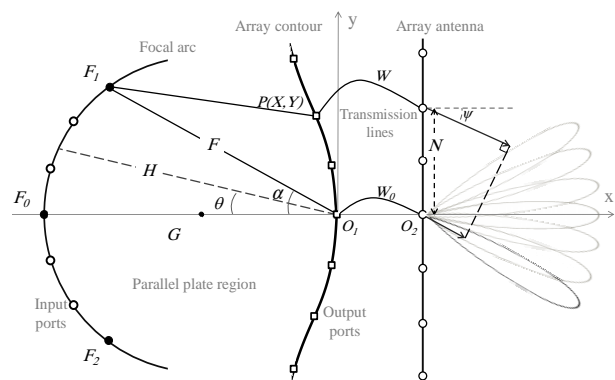


Fig. 1. Schematic of Rotman lens antenna and its parameters.

This paper is organized as follows. In Section 2, a basic overview of the Rotman lens design considerations is presented, and then it is discussed how to design the SIW Rotman lens, specifically. Also, an approach is explained to improve performance of the proposed SIW lens and the simulation results are represented. Section 3 deals with introducing the slot array antenna on SIW and designing a planar slot array for connecting to the Rotman lens. Simulation and measurement results of the Rotman lens in conjunction with the slot array antenna are shown and compared in Section 4. It is shown that the reflection coefficient of input ports, mutual coupling between them and all of the output patterns are appropriate in the whole frequency range.

## II. ROTMAN LENS DESIGN

### A. Rotman overview

As shown in Fig. 1, Rotman lens has two arcs that are called “focal arc” and “array contour”. The points of array contour are defined by  $P(X,Y)$  and connected to the array elements by lines with the length of  $W$ . Determining the number of array elements ( $NE$ ) and the distance between them ( $d$ ), considering the required scan angle, desired beamwidth and array element type, is the first step in lens designing. In second stage, some of the initial parameters of lens including  $\epsilon_r$  of the substrate, focal angle ( $\alpha$ ), beam angle corresponding to off axis focal point ( $\psi_\alpha$ ) and off axis to on axis focal length ( $G/F=g$ ) must be determined. The third step is calculation of normalized location of output ports of lens ( $x,y$ ) and normalized length of transmission lines ( $w$ ) by using design equations of Rotman and Turner’s paper [4]. According to this paper, ( $x,y$ ) coordinates and ( $w$ ) length, are calculated from the following equations:

$$x = \frac{-1}{(g-a)} \left( (g-1)w + 0.5\eta^2 b_1^2 \right), \quad (1)$$

$$y = \frac{b_1}{b_0} \eta (1-w), \quad (2)$$

$$aw^2 + bw + c = 0. \quad (3)$$

Where,  $\eta = N/F$  is the normalized coordinate of array elements relating to origin  $O_2$ , and  $a$ ,  $b$  and  $c$  are determined from [4]. In design equations, all dimensions are normalized to off axis focal length ( $F$ ), therefore all calculated parameters must be multiplied in  $F$  finally. The minimum amount of  $F$  is calculated from Equation (4).

$$F_{\min} = \frac{1}{\sqrt{\epsilon_r}} \frac{N_{\max}}{\eta_{\max}} = \frac{1}{\sqrt{\epsilon_r}} \frac{(NE-1)d}{2\eta_{\max}}. \quad (4)$$

According to Equation (4),  $\eta_{\max}$  must be chosen so that an appropriate value achieved for  $F$ , a large amount for  $F$ , enlarge the size of lens and increase the spillover and dielectric losses; on the other hand, according to Equation (5), the large amount of  $\eta_{\max}$  enhances the

aperture phase error. Thus, a trade off must be taken between them:

$$\Delta l = \frac{\Delta L}{F} = \left( h^2 + x^2 + y^2 + 2hx \cos \theta - 2hy \sin \theta \right)^{1/2} - h + w + \eta \sin \psi. \quad (5)$$

$h$ ,  $\theta$  and  $\psi$  are shown in Fig. 1.

### B. Implementing SIW Rotman lens

Before starting the SIW Rotman lens design, substrate integrated waveguide which is used as input and output ports and transmission lines should be designed at operating frequency. The SIW is in fact the fabrication of a metallic waveguide in the planar form. So, the SIW can be modeled with an equivalent dielectric filled waveguide [10]. The width of SIW ( $a_s$ ), for particular cutoff frequency is calculated from equation (6), in which the  $a_d$  is the width of equivalent waveguide with the same cutoff frequency,  $d$  is the diameter of via holes and  $p$  is the center to center distance of them:

$$a_d = a_s - 1.08 \frac{d^2}{p} + 0.1 \frac{d^2}{a_s}. \quad (6)$$

The proposed Rotman lens will operate at center frequency of 16 GHz and has 1 GHz bandwidth. Therefore to achieve appropriate dispersion characteristic in the entire band the width of equivalent waveguide is obtained  $a_d=8.5$  mm.  $d$  and  $p$  are chosen 0.5 mm and 0.8 mm, therefore the width of SIW can be calculated from Equation (6); i.e.,  $a_s=8.8$  mm.

Rotman lens design is started with selecting an appropriate substrate. In this project, Rotman lens is fabricated on Rogers RT/duroid 5880 substrate with  $\epsilon_r=2.2$  and 0.787 mm thickness. Based on the previous section, firstly, the number of array elements and the distance between them should be determined. In this lens we need to 7 beams at  $0^\circ$ ,  $\pm 10^\circ$ ,  $\pm 20^\circ$  and  $\pm 30^\circ$ , with a beamwidth of approximately  $15^\circ$  for each beam. To achieve these goals, based on linear array theory,  $NE$  and  $d$  should be chosen 7 and 10.7 mm, respectively. Now the initial value of design should be determined. To have a balanced lens with insignificant aperture phase error, we set  $\alpha=30^\circ$ ,  $\psi_\alpha=30^\circ$  and  $g=1.137$ . Since  $\alpha$  is equal to the  $\psi_\alpha$ , the input ports must located at angles of  $0^\circ$ ,  $\pm 10^\circ$ ,  $\pm 20^\circ$  and  $\pm 30^\circ$  on focal arc, in order to form the beams at the same angles.

The next step is the calculation of the normalized output ports coordinates and normalized transmission lines length by design Equations (1)-(3) in MATLAB software, and drawing the shape of the lens. In the following, the  $\Delta l$  is calculated and it is seen that the aperture error is acceptable for all elements of the array. Thus the values of  $\eta_{\max}$  and  $F$  are selected 0.75 and 54.6 mm, respectively. With possessing the focal length, the actual dimensions of Rotman lens are calculated. See Table 1 (because of the symmetry, the dimensions of

ports A5 to A7 are not mentioned). Design of the SIW transmission lines is the next step and is one of the most important steps of the design procedure. In SIW, Instead of creating phase difference by changing the length of transmission lines, the widths of lines must be changed [5]. The last step is to embed the dummy ports at blank spaces between input and output ports for eliminating the unwanted reflection from sides of the lens.

### C. Correction the lens shape

As already mentioned, the amplitude distribution of the array elements should be uniform, as far as possible. Incorrect design or improper orientation of input and output ports causes the low level amplitude at all of the array elements. But the low amplitude at one or several array elements is due to the poor design of dummy ports. In fact, the destructive interference of the direct and reflected waves at one or more output ports causes the amplitude of corresponding array elements to degrade. As a result, the orientation of input ports must be toward the central output port. This causes the mutual coupling between the input ports to be reduced; however, the amplitude level of the array elements to be increased. Also, to avoid undesired reflection in the transmission lines and to improve the amplitude and phase distribution of the array elements, the following points should be taken into account. The first, the transmission lines should have no bends as much as possible and the uniformity of them should be sustained. In addition, the dummy ports should be displaced slightly to the back due to decreasing the unwanted reflection from their metallic vias. Regarding to these points, the amplitude distribution of the array elements is achieved more uniform than previous works. The final scheme of Rotman lens is shown in Fig. 2.

### D. Results and analysis

All simulations are done by CST Microwave Studio full wave software using time domain solver. The amplitude and phase distributions of the array elements for frequencies of 15.5 GHz, 16 GHz and 16.5 GHz are plotted in Fig. 3 and Fig. 4. As can be observed the levels of amplitudes are appropriate, and the phase distributions are linear.

## III. PLANAR SLOT ARRAY ANTENNA

### A. Introduction of slot array

Due to the growing demand for the use of low weight and compact antennas, longitudinal shunt resonant slot array implemented on the SIW structure is

one of the most widely used antennas in radar and communication applications [11]. The design method of slot array on SIW is quite similar to those at the low height and dielectric filled metallic waveguide slot array one [12].

### B. Design of the slot array

To design each kind of slot array, two basic equations are used. These equations for longitudinal shunt resonant slot array on conventional waveguide, and low height and dielectric filled waveguide are presented in [11] and [12] respectively. As previously mentioned, the planar slot array has 7 SIW waveguides. The number of slots of each waveguide depends on the desirable bandwidth. In this work, 4 slots on each waveguide are appropriate. This number of slots is corresponding to 5% bandwidth at center frequency of 16 GHz. The amplitude distribution on all array elements is considered to be uniform, that leading to a pattern with approximately -13 dB SLL. Now the length and offset of all slots can be obtained by employing basic design equations of [12].

Table 1: Coordinates of the output ports and relative length of transmission lines of Rotman lens (in mm)

	A1	A2	A3	A4
X	-6.4	-2.9	-0.7	0
Y	27.6	18.3	9.2	0
W	-0.15	0.24	0.09	0

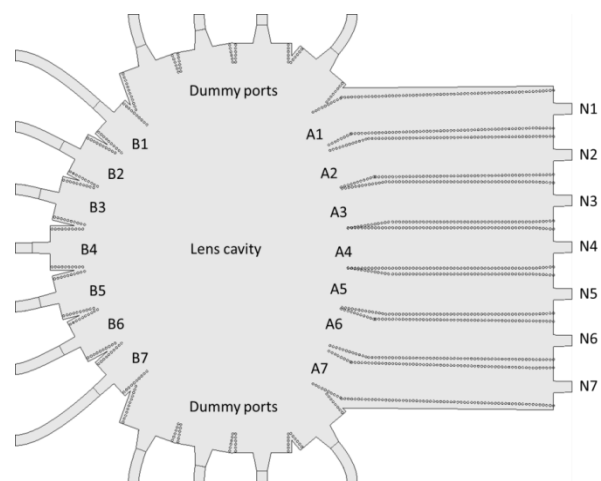


Fig. 2. Final scheme of the SIW Rotman lens. Input ports, output ports and array elements are named with B, A and N respectively.

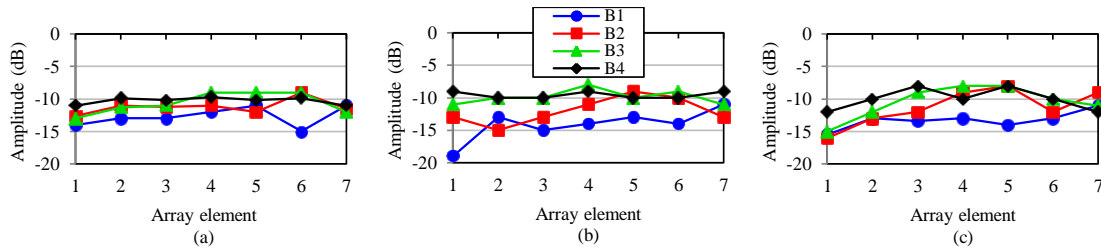


Fig. 3. Amplitude distribution of array elements for three frequencies: (a) 15.5 GHz, (b) 16 GHz, and (c) 16.5 GHz.

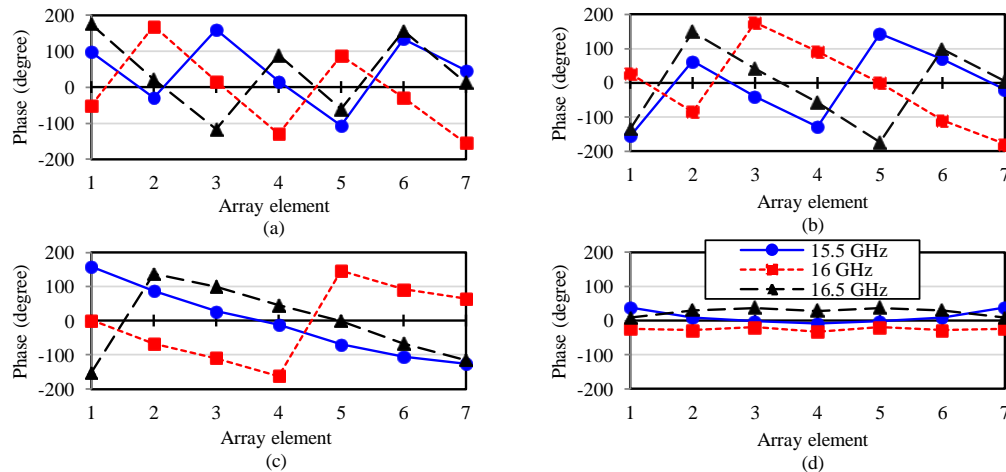


Fig. 4. Relative phase distribution of array elements for three frequencies when the beam ports: (a) B1, (b) B2, (c) B3, and (d) B4 are excited.

#### IV. INTEGRATING LENS AND SLOT ARRAY ANTENNA

The prototype of Rotman lens antenna that is the combination of Rotman lens and planar slot array is shown in Fig. 5 (a). The width and the length of antenna including connectors are 12.5 cm and 18.5 cm. As shown in Figs. 5 (a), (b), the scattering parameters of antenna are measured by a network analyzer, and during the measurement all ports except the ports under test were terminated with 50  $\Omega$  loads.

Figure 6 shows the measured reflection coefficients of all the input ports and also the mutual coupling between some of them. Inspection of Fig. 6 (a) reveals that, only the S44 exceeds the recommended limit -10 dB at high edge of the frequency range, and all the reflection coefficients are less than -10 dB. This occurs due to the smaller bandwidth of the slot array, which is from 15.5 to 16.3 GHz. The mutual coupling between other input ports is similar to those shown in Fig. 6 (b) and all of them are below -10 dB. The radiation patterns of input ports in E-plane (yoz) and radiation pattern of B4 in H-plane (xoz) at center frequency are simulated and measured at a microwave anechoic chamber. The simulated and measured patterns of ports B1 to B4 in E-plane are represented in Figs. 7 (a), (b) respectively. Because of the symmetry, the patterns of input ports B5

to B7 are not plotted. The SLL, HPBW, beam direction and gain of beams B1 to B4 in E-plane at center frequency are presented in Table 2.

Due to the true time delay property of Rotman lens, the characteristics of beams at the other frequencies of the band remain approximately unchanged. Also the simulated and measured co-pol and cross-pol radiation patterns of central port B4 in E-plane and H-plane are shown in Fig. 7 (b) and Fig. 8 respectively. This figure shows the low cross polarization level of the slot array antenna.

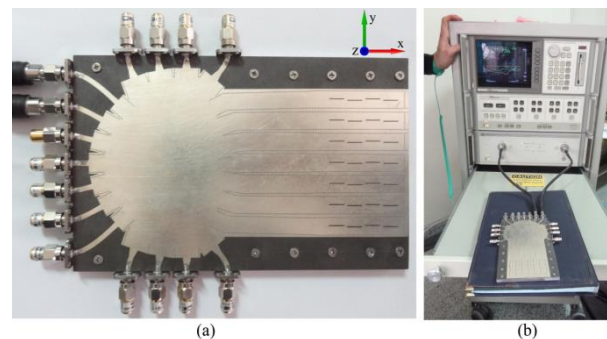


Fig. 5. (a) The prototype of Rotman lens with planar slot array antenna, and (b) scattering parameters measurement.

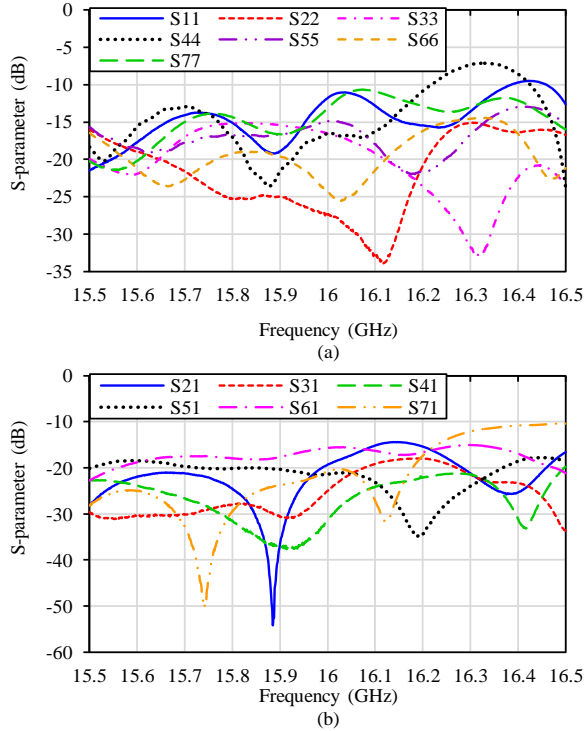


Fig. 6. Measured (a) reflection coefficients of all the input ports, and (b) mutual coupling between some of input ports.

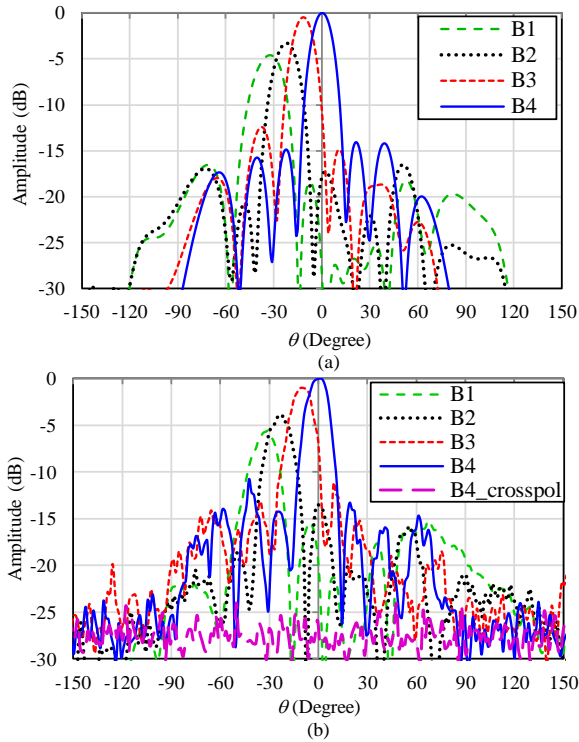


Fig. 7. (a) Simulated and (b) measured patterns of Rotman lens antenna in E-plane at center frequency.

Table 2: SLL, HPBW, beam direction and gain of beams B1 to B4 in E-plane at center frequency

	B1	B2	B3	B4
SLL (dB)	-10.2	-10	-10.3	-11
HPBW (deg)	16	17	15	14
Beam direction (deg)	31.1	21.4	10.7	0.3
Gain (dB)	10.6	12	15.1	16.5

The SLL and HPBW of beam B4 in H-plane at center frequency are -11.1 dB and 25°, respectively. The graph of simulated and measured gain versus frequency for port B4 is shown in Fig. 9. As can be observed, the gain is declined at the end of frequency range. This is also due to the lower bandwidth of the slot array antenna. Because of the errors of fabrication and measurement, the measured gain is usually less than simulated one.

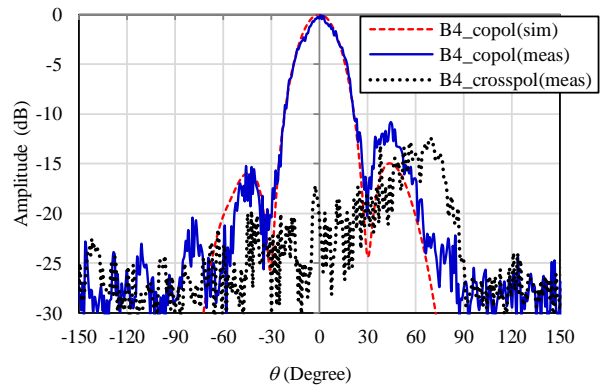


Fig. 8. Simulated and measured co-pol and cross-pol radiation patterns of B4 at center frequency in H-plane.

The SLL and HPBW of beam B4 in H-plane at center frequency are -11.1 dB and 25°, respectively. The graph of simulated and measured gain versus frequency for port B4 is shown in Fig. 9. As can be observed, the gain is declined at the end of frequency range. This is also due to the lower bandwidth of the slot array antenna. Because of the errors of fabrication and measurement, the measured gain is usually less than simulated one.

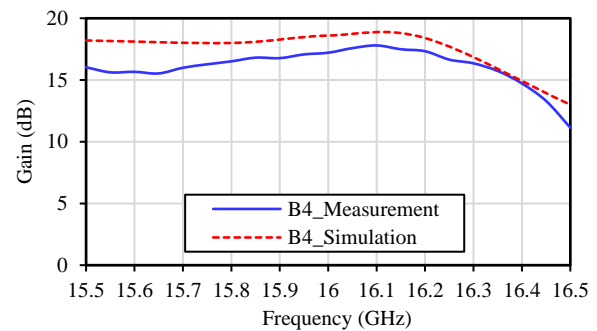


Fig. 9. Simulated and measured gain of input port B4 versus frequency.

## V. CONCLUSION

In this paper, a SIW Rotman lens antenna is designed and fabricated to use as a multi-beam antenna. This antenna is made from the integration of a Rotman lens and a planar slotted array antenna. The measured reflection coefficients of input ports and mutual coupling of them are below -10 dB in the range of 15.5 to 16.3 GHz. The simulated and measured patterns are in good agreement; and also the SLL, HPBW, gain and cross polarization are acceptable. This paper revealed that the SIW Rotman lens antenna is a good alternative for heavy and bulky metallic multi-beam antennas in aerial and satellite communication applications.

## ACKNOWLEDGMENT

The authors would like to thank Avionics Research Institute, Isfahan University of Technology, Iran to support of this project.

## REFERENCES

- [1] P.-C. Chiang, W.-J. Liao, Y.-T. Tu, and L. Hsin-Chin, "Implementation of direction-of-arrival estimation using rotman lens array antenna," in *Electromagnetic Theory (EMTS), Proceedings of 2013 URSI International Symposium on*, pp. 855-858, 2013.
- [2] R. C Hansen, *Phased Array Antennas*. New Jersey: Wiley & Sons, 2009.
- [3] S. Mubeen, A. M. Prasad, and A. J. Rani, "On the beam forming characteristics of linear array using nature inspired computing techniques," *ACES*, vol. 1, no. 6, 2016.
- [4] W. Rotman and R. Turner, "Wide-angle microwave lens for line source applications," *IEEE Trans. Antennas Propag.*, vol. 11, no. 6, pp. 623-632, Nov. 1963.
- [5] Y. J. Cheng, W. Hong, K. Wu, Z. Q. Kuai, C. Yu, J. X. Chen, J. Y. Zhou, and H. J. Tang, "Substrate integrated waveguide (SIW) Rotman lens and its Ka-band multibeam array antenna applications," *IEEE Trans. Antennas Propag.*, vol. 56, no. 8, pp. 2504-2513, Aug. 2008.
- [6] E. Sbarra, L. Marcaccioli, R. V. Gatti, and R. Sorrentino, "A novel Rotman lens in SIW technology," in *2007 European Radar Conference, EURAD*, pp. 236-239, 2007.
- [7] Z. X. Wang, D. P. Fan, and L. Z. You, "A design of microstrip Rotman lens," in *2012 International Conference on Microwave and Millimeter Wave Technology (ICMMT)*, pp. 1-4, 2012.
- [8] A. F. Peterson and E. O. Rausch, "Scattering matrix integral equation analysis for the design of a waveguide Rotman lens," *IEEE Trans. Antennas Propag.*, vol. 47, no. 5, pp. 870-878, May 1999.
- [9] S. A. R. Hosseini, Z. H. Firouzeh, and M. Maddahali, "Design of Rotman lens antenna at Ku-

band based on substrate integrated technology," *JCE*, vol. 3, no. 1, pp. 33-44, 2014.

- [10] F. Xu and K. Wu, "Guided-wave and leakage characteristics of substrate integrated waveguide," *IEEE Trans. Microw. Theory Tech.*, vol. 53, no. 1, pp. 66-73, Jan. 2005.
- [11] R. Elliott and L. Kurtz, "The design of small slot arrays," *IEEE Trans. Antennas Propag.*, vol. 26, no. 2, pp. 214-219, Mar. 1978.
- [12] R. Elliott and W. O'Loughlin, "The design of slot arrays including internal mutual coupling," *IEEE Trans. Antennas Propag.*, vol. 34, no. 9, pp. 1149-1154, Sep. 1986.



**Seyyed Alireza Hosseini** received the B.Sc. degree in Electronics and Telecommunications from Shahed University, Tehran, Iran, in 2011 and the M.Sc. degrees in Electrical Engineering from Isfahan University of Technology (IUT), Isfahan, Iran, in 2014. His research interests include slot array antennas, cavity filters, and phase array antennas.



**Zaker Hossein Firouzeh** received the B.Sc. degree in Electrical Engineering from Isfahan University of Technology (IUT), Isfahan, in 1999 and the M.Sc. and Ph.D. degrees in Electrical Engineering from Amirkabir University of Technology (AUT), Tehran, Iran, in 2002, and 2011, respectively. He is currently a Faculty Member at the Department of Electrical and Computer Engineering, Isfahan University of Technology. His current research interests include antenna design and measurements, numerical techniques in electromagnetics and EMC/EMI.



**Mohsen Maddahali** received the B.S. degree in Electronics and Telecommunications from Isfahan University of Technology (IUT), Isfahan, Iran, in 2005 and the M.S. and Ph.D. degrees in Electrical Engineering from Tarbiat Modares University, Tehran, Iran, in 2008 and 2012, respectively. Since 2012, he has been an Assistant Professor with the Department of Electrical and Computer Engineering, IUT. His research interests include computational electromagnetism, waveguide slot antenna design, and phase array antennas.